

Different histological subtypes of parotid gland tumors: CT findings and diagnostic strategy

Zhi-Feng Xu, Fang Yong, Tian Yu, Ying-Yu Chen, Qiang Gao, Tao Zhou, Ai-Zhen Pan, Ren-Hua Wu

Zhi-Feng Xu, Fang Yong, Tian Yu, Ying-Yu Chen, Qiang Gao, Tao Zhou, Ai-Zhen Pan, Department of Radiology, the First People's Hospital of Foshan, Foshan 528000, Guangdong Province, China

Ren-Hua Wu, Department of Radiology, the Second Affiliated Hospital, Medical College of Shantou University, Shantou 515041, Guangdong Province, China

Author contributions: Xu ZF performed the majority of experiments and wrote the manuscript; Yong F, Yu T and Chen YY collected the data and analyzed images; Gao Q and Zhou T prepared the graphs; Pan AZ designed the study; and Wu RH was involved in editing the manuscript.

Correspondence to: Ai-Zhen Pan, MD, Department of Radiology, the First People's Hospital of Foshan, Foshan 528000, Guangdong Province, China. pazhen2121@126.com

Telephone: +86-757-83162121 Fax: +86-757-83162121

Received: March 13, 2013 Revised: July 16, 2013

Accepted: July 30, 2013

Published online: August 28, 2013

Abstract

AIM: To present computed tomography (CT) findings of different histological subtypes of parotid gland masses in detail and to establish diagnostic strategy.

METHODS: From January 2009 to November 2011, 56 patients were collected through the histopathology and Picture Archiving and Communication Systems records, which revealed 5 basal cell adenoma (BCA), 16 pleomorphic adenoma (PA), 25 Warthin's tumor (War-T), 3 Kimura's disease (KD) and 7 parotid carcinoma (PCa) cases. All the CT images were retrospectively analyzed by two radiologists in consensus, based on their description of morphology (location, number, size, margin and fibrous capsule) and enhancement patterns of masses. In addition, the diagnostic efficiency of diagnostic strategy is tested.

RESULTS: War-T and BCA patients' mean age was 59.9 ± 12.6 years and 58.4 ± 18.2 years; the significant dif-

ference was seen in War-T vs PA and BCA vs PA. About 40% of War-Ts presented with bilateral multifocal lesions, a higher ratio than others. Seventy two percent of War-Ts were limited to the superficial lobe, followed by BCA 60% and PA 40%. Vessel facing sign and enlarged lymph nodes were both frequent in War-T, which respectively accounts for 84% and 76% of cases. Rapid contrast enhancement and decreases were unique for War-T. BCA and PA showed obvious delayed enhancement. The diagnostic strategy of parotid gland tumor had a good diagnostic efficiency, with high accuracy, sensitivity and specificity.

CONCLUSION: Determination of the histological subtypes of parotid gland masses might be possible based on CT findings and clinical data. A diagnostic strategy with high diagnostic efficiency was established.

© 2013 Baishideng. All rights reserved.

Key words: Parotid gland tumor; Pleomorphic adenoma; Warthin's tumor; Multi slice computed tomography

Core tip: In this study, the key computed tomography findings of different histological subtypes of parotid gland masses were summarized in detail and a diagnostic strategy with high diagnostic efficiency was established.

Xu ZF, Yong F, Yu T, Chen YY, Gao Q, Zhou T, Pan AZ, Wu RH. Different histological subtypes of parotid gland tumors: CT findings and diagnostic strategy. *World J Radiol* 2013; 5(8): 313-320 Available from: URL: <http://www.wjgnet.com/1949-8470/full/v5/i8/313.htm> DOI: <http://dx.doi.org/10.4329/wjr.v5.i8.313>

INTRODUCTION

Salivary gland tumors (SGT) consist of a group of heterogeneous lesions with complex clinicopathological char-

acteristics and distinct biological behaviors, most of them arising in the parotid gland^[1]. Differentiation between a benign or malignant lesion and determination of the exact histological subtype are very difficult. Clinically, they usually present as a painless palpable mass, indistinguishable from the subtypes of SGTs, including pleomorphic adenoma (PA), basal cell adenoma (BCA), Warthin's tumor (War-T), parotid carcinoma (PCa) and Kimura's disease (KD). The risk for local recurrence is approximately 2% in War-T treated by enucleation, but the risk is approximately 85% for PA^[2,3]. Therefore, most important for choosing the appropriate surgical approach is the differentiation between a benign or malignant lesion, as well as the determination of the exact histological subtype. Fine needle aspiration biopsy (FNAB) proved to be a useful and reliable tool in the preoperative diagnosis of SGT^[4,5]. However, differentiation of a few benign and malignant lesions might be not only difficult but also impossible by only depending on FNAB. For instance, PA of variable histological patterns and adenoid cystic carcinoma, as well as BCA, can be mistaken^[6,7].

Ultrasound is most commonly used in parotid tumor diagnosis^[8-10], but it is weak for detecting masses located in the deep lobe and the results are closely related to the operator experience and skill level. Recently, magnetic resonance (MR) and computed tomography (CT) imaging-based techniques have been evaluated for the diagnosis of benign and malignant SGTs^[10-14]. In contrast to FNAB, MRI and CT noninvasive examination might provide a diagnosis and the range of tumor. MR image-based techniques, diffusion-weighted imaging (DWI) seems to have the highest potential to determine different histological subtypes non-invasively^[11,12,15]. Nevertheless, its disadvantages are limited availability, high cost and the long time needed. Patients with certain pacemakers or implanted metals cannot have magnetic resonance imaging. Previous CT imaging-based research was focused on the morphological characteristics, such as margin, size, location and density, with some studies involved in enhancement, but results were inconsistent and no diagnostic strategy has been established for benign and malignant lesion diagnosis^[9,13,16], much less the determination of the histological subtypes.

The objective of our study was to investigate the potential of CT imaging-based technology in differentiating various entities of parotid gland tumors by comprehensive analysis of the CT findings and clinical situation. Critical focus areas of CT imaging, such as location, number, margin, side, especially the vessel facing sign and enlarged lymph nodes around the lesions, and the enhancement features, were examined.

MATERIALS AND METHODS

Patient cohort and CT acquisition

Fifty-six patients with parotid gland tumor (diameter is < 3 cm) were enrolled in this study, which revealed 5 BCA, 16 PA, 25 War-T, 3 KD and 7 PCa cases. CT was

performed by using GE 64 light speed CT and Philips 256 iCT. The key CT parameters and scanning processes are summarized as follows: slice thickness 3-5 mm, pitch 1.375; effective exposure 240 mA at 120 kVp. Unenhanced CT was obtained throughout the entire neck and 1.5-2.0 mL/kg of nonionic contrast material (370 mg of iodine per milliliter) was injected in 30 s by use of a power injector. Arterial phase scan was acquired at 25 s after contrast agent injection and the vein phase scan was obtained at 60 s. In all patients, a parotid gland tumor was histologically proven by surgery before initiation of the therapy. The local ethics committee approved the study protocol and written informed consent was obtained from all patients before CT scan.

Image and data analysis

All images were reviewed on the Picture Archiving and Communication Systems by two radiologists respectively, and the morphological and enhancement patterns of lesions were depicted. Tumor location was defined as involving the superficial, deep, or both in the parotid gland. The tumor size was expressed in terms of maximal axial dimensions measured to the nearest millimeter (the largest lesion was measured in cases of multifocal lesions). The tumor was deemed to have a sharp margin if it was well-demarcated throughout its circumference and to have indistinct margins otherwise. For assessment of the attenuations of the tumors, a circular region of interest (ROI) excluded obvious cystic and necrotic areas. The enhancement pattern was categorized as either homogeneous or inhomogeneous. A tumor that showed inhomogeneous enhancement was further described as demonstrating either a non-enhancing curvilinear cleft or a cystic component. Some cases underwent two phases of scanning and the attenuation changes were calculated. Vessel facing sign and enlarged lymph nodes were also described for diagnosis. Here, vessel facing sign was referred to as small newborn blood vessels around tumors and the lymph node around the mass was defined as enlarged when its size was ≥ 5 mm.

In order to test the diagnostic efficiency of the diagnostic strategy, a new group of cases of parotid gland tumors were collected, including 12 War-T, 10 PA, 7 BCA and 5 PCa cases. The radiologist did not know the pathology results before analyzing the CT images and making a diagnosis. To evaluate the diagnostic efficiency, the accuracy, sensitivity and specificity of each subtype tumor diagnosis by using the diagnostic strategy advanced in this article was calculated.

Statistical analysis

All statistical analyses were computed with the Statistical Package for the Social Sciences, Version 13.0 (SPSS, Chicago, IL). The χ^2 test was used for the statistical analysis of differences in age, arterial phase strengthen rate and un-enhanced attenuation among the parotid gland nodules. The Mann-Whitney test was used for comparison between two groups. The level of signifi-

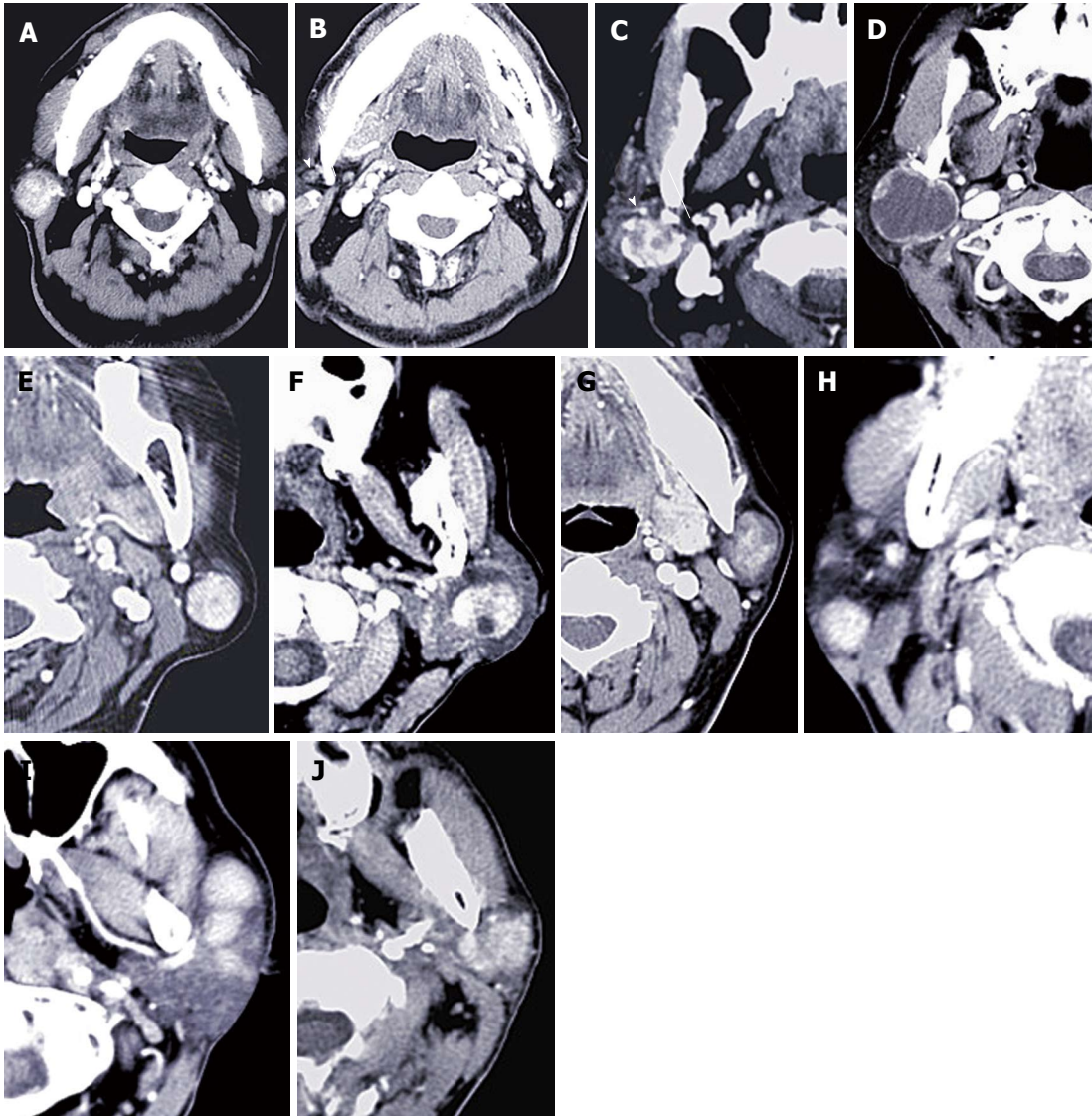


Figure 1 Computed tomography features of all observed subtypes of parotid gland tumors. A-D: Warthin's tumors (War-Ts) showing heterogeneous and apparent enhancement; A, B: bilateral multiple lesions with and enlarged lymph nodes; C: Tumors with multiple capsules and vessel facing sign; D: War-T had a large cystic degeneration; E, F: Basal cell adenoma showing apparent heterogeneous enhancement, with multiple low-density areas (E) and multiple capsules (F); G: Pleomorphic adenoma with apparent heterogeneous enhancement at 60 s; H, I: EG presenting unilateral multiple lesions with enlarged lymph nodes, well margin and homogenous enhancement; J: Parotid carcinoma displayed unclear margin and heterogeneous enhancement and involved the superficial and deep lobe.

cance was set at 5% ($P < 0.05$).

RESULTS

Clinical presentations

Table 1 shows the age, sex distribution and the radiological features of the masses. The War-T and BCA patient's mean age (War-T: 59.9 ± 12.6 years and BCA: 58.4 ± 18.2 years) were both much older than that of other subtypes. The significant difference was seen between War-T and PA, and also between BCA and PA. War-T and PCa frequently occur in males (male *vs* female was 7.3:1 and 4:1, respectively), whereas, BCA was predominant in females. Twenty of 25 patients with War-T were smokers, accounting for 80%, which was the highest among all subtypes of parotid masses.

Multi slice CT finding of subtypes of parotid glands tumors

Multi slice CT (MSCT) revealed a unilateral solitary tumor in all PCa and KD cases, and synchronous bilateral multifocal tumors in 10 War-T cases, which was the only disease that presented with bilateral lesions (Figure 1). Furthermore, for unilateral solitary tumors, PA and War-T occurred predominantly in the left side. Tumors limited to the superficial lobe of the parotid gland presented in 18 (72%) War-T, 6 (40%) PA, 3 (60%) BCA and 2 (33.3%) PCa cases. The proportion of War-T ranked first. The maximum axial diameter of the tumors exceeded 2 cm in the War-T and PA groups, with a mean of 2.2 ± 0.9 cm and 2.1 ± 0.73 cm, but there was no statistical difference. All KD cases had multiple lesions and a sharp margin, but 12 (80%) of PA cases had an unclear margin. Besides, the majority of tumors had a sharp

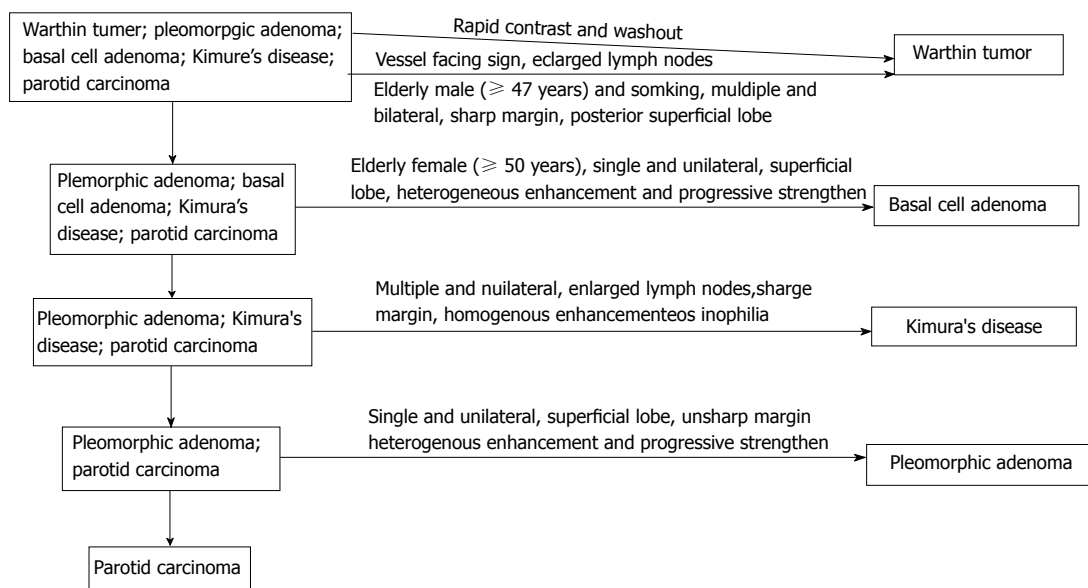


Figure 2 Time and computed tomography number curve of dual-phase contrast enhanced spiral computed tomography in the observed entities.

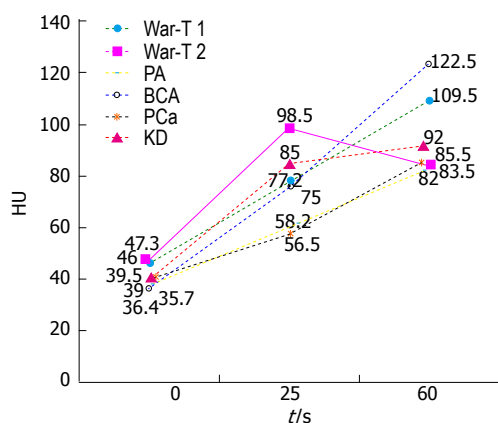


Figure 3 Diagnostic strategy of parotid gland tumors. War-T: Warthin's tumor; PA: Pleomorphic adenoma; BCA: basal cell adenoma; PCa: Parotid carcinoma; KD: Kimura's disease; HU: Unenhanced-attenuation.

margin in the War-T (84%) and BCA (80%) cases.

All BCA and PA cases and 19 (76%) War-T cases showed heterogeneous enhancement. Whereas, all masses in the KD group had homogeneous enhancement. None of the tumors demonstrated calcification, excluding one PA case with mottling calcification. Here, vessel facing sign was found in 21 War-T cases (Figure 1C), accounting for 84% in the War-T group. Twenty seven War-T cases had enlarged lymph nodes around the masses; among them, 8 cases were identified by histopathology and the rest were confirmed by two radiologists with abundant clinical experience. For tumors associated with enlarged lymph nodes, the proportion in the top two subtypes was KD (100%) and War-T (76%) (Figure 1B and H).

Among all tumor entities, War-T had the highest unenhanced attenuation value (49.0 ± 10.3 HU). When the un-enhanced attenuation values exceeded 45 HU, it strongly suggested a War-T diagnosis. Among all the parotid gland tumors patients, 13 War-T, 5 PA, 4 BCA, 3

KD and 4 PCa cases underwent double period scanning. Therefore, the dynamic change curve of the attenuation for each group was established according to average value (Figure 2). Four War-T cases presented with rapid contrast enhancement and rapid decrease. Nine War-T cases and other subtype lesions all showed increased enhancement and War-T and BCA cases were much more remarkable.

Diagnostic strategy

A diagnostic strategy for parotid gland tumor diagnosis was established initially according to the CT findings and clinical data analysis and is summarized in Figure 3. The efficiency of diagnostic strategy was very high in the subtypes of parotid gland tumor diagnosis. Table 2 shows the sensitivity, specificity and accuracy.

DISCUSSION

Relationship of clinical data to subtypes of parotid masses

Sex and age were always evaluated as useful information for benign or malignant tumors differentiation as well as histological type diagnosis. With respect to sex distribution, many previous reports have described a female predominance in BCA and PA, while males frequently predominate in War-T^[14,17,18]. Our study demonstrated similar results, with a male: female ratio of 7.3: 1 for War-T, a male: female ratio of 1:4 for BCA and of 1:1.5 for PA. The average age of cases with War-T and BCA have been reported to be approximately 57 and 59 years^[19,20], a decade older than those with PA. Our results are similar to the previous viewpoints. In this study, 80% of War-T cases were smokers, the highest percentage among all subtypes. It emphasized the fact that smoking is an etiological factor in War-T development^[21,22]. To summarize, it is useful to know age, sex and smoking for parotid gland tumor diagnosis, especially for War-T and BCA.

Table 1 Clinical and radiological features of Warthin’s tumors, pleomorphic adenomas, basal cell adenoma and malignant tumors *n* (%)

Features	War-T	PA	BCA	KD	PCa
No. of patients	25	15	5	3	6
Age(yr)(mean ± SD)	59.9 ± 12.6	41.3 ± 11.4	58.4 ± 18.2	48 ± 15.8	51.3 ± 17.1
Sex ratio (male: female)	7.3:1	1:1.5	1:4	2:1	4:1
Smoking (yes: no)	4:1	1.5:1	0.7:1	2:1	2:1
Single: multiple lesions	1.5:1	6.5:1	5:0	0:3	6:0
Side (right: left: bilateral)	4:11:10	4:11:0	2:3:0	2:1:0	2:4:0
Location(superficial-lobe (posterior-inferior portion): deep-lobe: both)	18 (17):0:7	6 (2):3:6	3 (2):0:2	0:0:3	2 (0):0:4
Size (cm) (mean ± SD)	2.2 ± 0.91	2.1 ± 0.73	1.7 ± 0.38	1.7 ± 0.59	1.6 ± 0.32
Margin(clear: unclear)	5.3:1	1:4	4:1	3:0	1:1
Density (homogenous: heterogeneous)	1.3:2	0:15	0:5	3:0	1:1
Vessel facing sign	21 (84)	2 (13.3)	1 (20)	0 (0)	0 (0)
Enlarged lymph nodes	19 (76)	2 (13.3)	1 (20)	3 (100)	2 (33.3)
Unenhanced-attenuation (HU)	49.0 ± 10.3	39.5 ± 7.5	35.7 ± 0.9	38.0 ± 3.0	39.8 ± 6.2

PA: Pleomorphic adenoma; BCA: Basal cell adenoma; War-T: Warthin’s tumor; PCa: Parotid carcinoma; KD: Kimura’s disease; AP: Arterial phase.

Table 2 Diagnostic efficiency of diagnostic strategy for each subtype diagnosis, the sensitivity, specificity and accuracy were evaluated

	Warthin’s tumor	Pleomorphic adenoma	Basal cell adenoma	Parotid carcinoma
Sensitivity	100%	90.0%	71.4%	80.0%
Specificity	95.5%	83.3%	96.4%	89.7%
Accuracy	97.1%	85.3%	94.1%	88.2%

MSCT findings for subtypes of parotid masses diagnosis

Calcification is rare in parotid tumors. In our research, small mottling calcification was solely observed in one PA patient. We speculated it was related to ossification. In this study, about 40% of War-T cases were multiple and bilateral. Additionally, in 94.4 % of War-T cases, the masses located in the superficial lobe were limited in the posterior and inferior quadrant, much higher than any other subtypes. These results are in agreement with the previous study^[13,17,18,23]. Posterior and inferior quadrants of parotid gland superficial lobe with rich lymphatic organization were the most frequent site of War-T. It demonstrated that War-T likely arises from lymph nodes and the heterotopic salivary gland tissue’s nearby lymph nodes^[24,25]. Additionally, PA and PCa all presented with single and unilateral lesions. Therefore, a tumor is strongly considered as War-T when it presents with multiple and bilateral lesions and the lesions are located in the posterior and inferior quadrant of the superficial lobe.

According to previous reports, cyst formation is a main histopathological feature for BCA and War-T, especially for BCA, presenting in more than one half of tumors examined (65%)^[9,13,26]. In this study, 76% (19/25) of War-T cases and all BCA cases showed markedly inhomogeneous enhancement. However, only 7 (28%) War-T cases and 1 (20%) BCA case had a distinct cystic component, lower than previous reports. We speculated that the cyst was so small that it merely displayed a low density zone on CT imaging. All PA in our study showed inhomogeneous enhancement which might be due to PA being comprised of mixed components.

Vessel facing sign is defined as the posterior mandible veins near to the tumor and it was reported in favor of War-T^[27]. However, it is associated with tumor size and sick time. Therefore, our view was that the vessel facing sign advanced before was not significant for War-T diagnosis. In this study, vessel facing sign was defined as increased new blood vessels next to the tumor. It should better reflect the biological behavior and histopathological features. Eighty four percent of War-T cases presented with vessel facing sign and was much higher than other entities, accounting for 87.5% of all cases with vessel facing sign. Enlarged lymph nodes might be firstly advanced as a sign for differential diagnosis in this study. Here, the enlarged lymph nodes were defined as the diameter ≥ 5mm. The results indicated that all KD cases and 76% (19/25) of War-T cases had enlarged lymph nodes. We speculated that the following reasons might give a explanation: (1) The lymphatic organization is frequently involved by KD itself; (2) Large number of lymphocytes are tightly arranged in the mesenchymal stroma of War-T and with a lymphatic biochemical center^[24,28-30]. Therefore, an inflammatory reaction occurs frequently and causes reactive lymph node hyperplasia; and (3) The enlarged lymph nodes might be the lesion itself because War-T was considered to arise from lymph nodes. In summary, the vessel facing sign and enlarged lymph nodes strongly indicate War-T.

In general, BCA are usually assumed to be rather small tumors, less than 3 cm in their greatest dimension, and smaller than War-T and PA^[11,18]. The same trend was also seen in our study but no significant difference was seen between any two entities. In addition, the size was the smallest in the PCa cases. It is a little controversial as the smaller the tumor, the more likely it is to be malignant; of course, more evidence is needed. Whether a tumor had a sharp margin or not was usually considered as a sign for benign or malignant lesion differentiation, but it is still a continuing controversy. Sharafuddin *et al*^[31] and Som *et al*^[32] advanced that an unsharp margin was the reliable phenomenon for malignancy. In contrast, Freling *et al*^[33] dem-

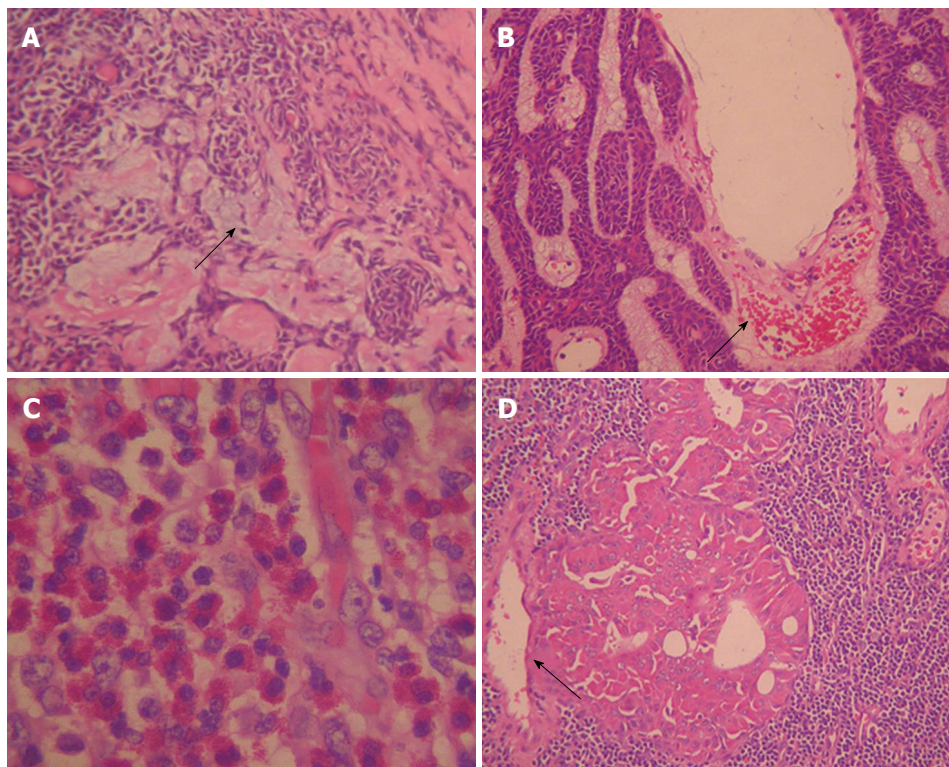


Figure 4 Histopathological features of pleomorphic adenoma, basal cell adenoma, Kimura's disease and Warthin's tumor (HE staining, x 400). A: Pleomorphic adenoma are a large amount of myxoid matrix (arrow), rare epithelial components, and low micro vessel count; B, D: Basal cell adenoma and Warthin's tumor (War-T) respectively, small capillaries and venules are prominent (black arrow). War-T consists of abundant lymphoid interstitial tissue and gland tube sample structures; C: Kimura's disease demonstrates a lot of eosinophil invasion.

onstrated only about 50% of sharp margin lesions were malignant lesions. Our results showed that 84% (21/25) of War-T cases and 80% (4/5) of BCA cases had a sharp margin, much higher than that of PCa (50%). It agreed with Som *et al*^[32] who strongly suggested that a sharp margin was associated with a benign tumor. However, 80% of PA cases had an unsharp margin. Histopathologically, War-T and BCA had an intact capsule, but PA had an incomplete coated capsule which might be the main reason explaining the different margin display. KD as a chronic granulomatous lesion with superficial lymph nodes and soft tissue involved usually presented a mass with an unsharp margin. However, all KD cases displayed a sharp margin in our study (Figure 4C), which might be due to focusing on the smaller nodules, with the largest diameter less than 2 cm.

The contrast enhancement features of parotid tumors are related to their histopathological features and vascular architecture. Histopathologically, most War-T cases have a high micro-vessel count and high cellularity, and BCA have characteristic numerous endothelium-lined vascular channels, in which small capillaries and venules are prominent^[20,34] (Figure 4B and D). The characteristic dynamic CT findings of War-T and BCA are rapid contrast enhancement at the arterial phase and War-T decreases enhancement at the venous phase, while BCA continues to strengthen. BCA showed lower enhancement than War-T and KD, but was higher than PCa and PA at the arterial phase and displayed the highest strength at 60 s. These results were in agreement with the above-mentioned previous study^[13,14,35]. Surprisingly, 9 War-T cases demonstrated progressive strengthening, similar to the enhancement pattern of BCA, but its attenuation at 60 s phase was less than BCA. However, it has been reported that some

War-T exhibited slow washout and displayed a steady level enhancement^[20]. Tumors with cystic changes and low cellularity are the main explanation for it. However, so far, no report demonstrated that War-T presented progressive strengthening but what is responsible for this finding is still unknown. Anyway, the rapid increase and decreases curve strongly suggest a War-T diagnosis, but not for all War-T.

The typical histopathological features of PA are a large amount of myxoid matrix, rare epithelial components, and a low micro-vessel count (Figure 4A). Previous reports have indicated that these tumors enhance gradually. All PA in our study were enhanced gradually, similar to the previous reports^[13,20,35,36]. We speculate that the gradual enhancement might be attributed to the slow leakage of contrast material to vascular spaces and myxoid matrix from the low number of micro-vessels. The enhanced pattern of PCa was similar to PA, which also presented with gradual enhancement. KD cases were rapid contrast enhancement in the arterial phase and displayed a steady level enhancement. We guess that the difference was based on the histopathology. War-T and PCa usually have a high micro-vessel count, but the micro-vessels in PCa were immature, inflexible and circuitous, which may lead to lowering the contrast speed. Whereas, PA had a lack of micro-vessels, PA and PCa were impossible to distinguish in two phase enhancement.

Diagnostic strategy

Here, a diagnostic strategy for parotid gland tumor diagnosis was advanced initially in our study, according to the CT findings and clinical data analysis and summary. For subtypes of parotid gland mass diagnosis and differentiation, some diagnostic key points were summarized but the key points of

how to use it for each subtype diagnosis were not advanced in detail and their diagnosis efficiency were not distinguished separately. At present, in the diagnostic strategy, all the key points should be comprehensively analyzed before making a conclusion and the exclusive method is very important. In addition, new viewpoints were advanced and used in this strategy, such as the vessel facing sign and enlarged lymph nodes. In this study, the vessel facing sign was defined as increased new blood vessels next to the tumor. The enlarged lymph nodes were defined as the diameter ≥ 5 mm.

We found that the efficiency of diagnostic strategy was very high. For War-T diagnosis, the sensitivity, specificity and accuracy all exceeded 95%; moreover, the sensitivity reached 100%. It had a high specificity and accuracy, 96.4% and 94.1%, respectively, for BCA diagnosis. In addition, for PA and PCa diagnosis, the sensitivity, specificity and accuracy all exceeded 80%. Our results showed that the diagnostic strategy, advanced firstly in our study, might be a robust tool for subtype parotid gland tumor diagnosis. However, it is still preliminary and needs to be improved.

In summary, War-T, PA, BCA, KD and PCa have their features on CT images and clinical manifestation. A combined clinical and radiological assessment of a patient is essential in establishing an accurate diagnosis. Contrast material enhanced CT, especially the dynamic enhanced scanning, is essential for differential diagnosis. The diagnostic strategy of parotid gland tumors was established successfully and is a good strategy with high diagnostic efficiency.

COMMENTS

Background

Determination of the exact histological subtype of parotid gland tumors (PGT) is very important for the appropriate surgical approach. Fine needle aspiration biopsy (FNAB) is the gold standard for diagnosis but differentiation of a few benign and malignant lesions is still difficult. In contrast to FNAB, computed tomography (CT) noninvasive examination might provide a diagnosis and the range of tumor. Previous CT imaging-based research was focused on the morphological characteristics, with some studies involved in enhancement, but results were inconsistent and no diagnostic strategy has been established. In this study, the CT findings of various entities of PGTs were summarized and a diagnostic strategy was tried to be established.

Research frontiers

Parotid gland tumors consist of a group of heterogeneous lesions with complex clinicopathological characteristics and distinct biological behaviors. Before surgery, it is very important to determine the exact histological subtypes. This study tried to depict and summarize the multi slice CT (MSCT) features of pleomorphic adenoma (PA), basal cell adenoma (BCA) and Warthin's tumor (War-T) in detail. Meanwhile, the authors try to establish a good diagnostic strategy with high diagnostic efficiency.

Innovations and breakthroughs

Ultrasound is still the first choice for parotid tumor diagnosis, but here MSCT findings were depicted and summarized. Previous MSCT imaging-based research was usually focused on the morphological characteristics and enhancement pattern, but the results were different. Now a diagnostic strategy for differential diagnosis has been advanced. In this study, the various entities of PGTs, MSCT findings and clinical situation were depicted in detail. Critical focus areas of CT imaging, such as location, number, margin, side, especially the vessel facing sign and enlarged lymph nodes around the lesions and the enhancement features, were examined. Here, in order to offer better information to reflect a lesion's biological behavior and histopathological features, the vessel facing sign was redefined as increased new blood vessels next to the tumor. In addition, enlarged lymph nodes were firstly advanced as a sign for differential diagnosis. The most important was that a good diagnostic strategy with high diagnostic efficiency was

established. For War-T diagnosis, the sensitivity, specificity and accuracy all exceeded 95%; moreover, the sensitivity reached 100%. It had a high specificity and accuracy, 96.4% and 94.1% respectively, for BCA diagnosis.

Applications

The study results suggest that determination of the histological subtypes of parotid gland masses might be possible based on CT findings and clinical data. A good diagnostic strategy was necessary.

Terminology

War-T: A benign tumor in the salivary gland, almost all in the parotid gland. Vessel facing sign: Vessel facing sign was defined as the blood vessels next to tumor.

Peer review

The authors have prepared a very well done study, correlating histological subtypes of parotid gland tumors to CT findings. They collected data on 56 patients with firm histopathological analysis. The War-T type cases demonstrated rapid contrast enhancement followed by a decrease in the same. BCA has delayed enhancement. Thus, it is conceivable that CT could be used to help to diagnosis the histological subtype of the parotid gland tumors. The methods are well detailed and the discussion is fairly thorough. A good diagnostic strategy was advanced.

REFERENCES

- 1 **Tian Z**, Li L, Wang L, Hu Y, Li J. Salivary gland neoplasms in oral and maxillofacial regions: a 23-year retrospective study of 6982 cases in an eastern Chinese population. *Int J Oral Maxillofac Surg* 2010; **39**: 235-242 [PMID: 19951834 DOI: 10.1016/j.ijom.2009.10.016]
- 2 **Schindler S**, Nayar R, Dutra J, Bedrossian CW. Diagnostic challenges in aspiration cytology of the salivary glands. *Semin Diagn Pathol* 2001; **18**: 124-146 [PMID: 11403256]
- 3 **Witt RL**. The significance of the margin in parotid surgery for pleomorphic adenoma. *Laryngoscope* 2002; **112**: 2141-2154 [PMID: 12461331 DOI: 10.1097/00005537-200212000-00004]
- 4 **Layfield LJ**. Fine-needle aspiration in the diagnosis of head and neck lesions: a review and discussion of problems in differential diagnosis. *Diagn Cytopathol* 2007; **35**: 798-805 [PMID: 18008348 DOI: 10.1002/dc.20769]
- 5 **Tatomirovic Z**, Skuletic V, Bokun R, Trimcev J, Radic O, Cerovic S, Strbac M, Zolotarevski L, Tukic Lj, Stamatovic D, Tarabar O. Fine needle aspiration cytology in the diagnosis of head and neck masses: accuracy and diagnostic problems. *J BUON* 2009; **14**: 653-659 [PMID: 20148458]
- 6 **Das DK**, Petkar MA, Al-Mane NM, Sheikh ZA, Mallik MK, Anim JT. Role of fine needle aspiration cytology in the diagnosis of swellings in the salivary gland regions: a study of 712 cases. *Med Princ Pract* 2004; **13**: 95-106 [PMID: 14755143 DOI: 10.1159/000075637]
- 7 **Behzatoğlu K**, Bahadır B, Kaplan HH, Yücel Z, Durak H, Bozkurt ER. Fine needle aspiration biopsy of the parotid gland. Diagnostic problems and 2 uncommon cases. *Acta Cytol* 2004; **48**: 149-154 [PMID: 15085745]
- 8 **Brennan PA**, Herd MK, Howlett DC, Gibson D, Oeppen RS. Is ultrasound alone sufficient for imaging superficial lobe benign parotid tumours before surgery? *Br J Oral Maxillofac Surg* 2012; **50**: 333-337 [PMID: 21371794 DOI: 10.1016/j.bjoms.2011.01.018]
- 9 **Shi L**, Wang YX, Yu C, Zhao F, Kuang PD, Shao GL. CT and ultrasound features of basal cell adenoma of the parotid gland: a report of 22 cases with pathologic correlation. *AJNR Am J Neuroradiol* 2012; **33**: 434-438 [PMID: 22194377 DOI: 10.3174/ajnr.A2807]
- 10 **de Ru JA**, van Leeuwen MS, van Benthem PP, Velthuis BK, Sie-Go DM, Hordijk GJ. Do magnetic resonance imaging and ultrasound add anything to the preoperative workup of parotid gland tumors? *J Oral Maxillofac Surg* 2007; **65**: 945-952 [PMID: 17448846 DOI: 10.1016/j.joms.2006.04.046]
- 11 **Habermann CR**, Arndt C, Graessner J, Diestel L, Petersen KU, Reitmeier F, Ussmueller JO, Adam G, Jaehne M. Diffusion-weighted echo-planar MR imaging of primary parotid gland tumors: is a prediction of different histologic subtypes

- possible? *AJNR Am J Neuroradiol* 2009; **30**: 591-596 [PMID: 19131405 DOI: 10.3174/ajnr.A1412]
- 12 **Yabuuchi H**, Matsuo Y, Kamitani T, Setoguchi T, Okafuji T, Soeda H, Sakai S, Hatakenaka M, Nakashima T, Oda Y, Honda H. Parotid gland tumors: can addition of diffusion-weighted MR imaging to dynamic contrast-enhanced MR imaging improve diagnostic accuracy in characterization? *Radiology* 2008; **249**: 909-916 [PMID: 18941162 DOI: 10.1148/radiol]
 - 13 **Yerli H**, Aydin E, Coskun M, Geyik E, Ozluoglu LN, Haberal N, Kaskati T. Dynamic multislice computed tomography findings for parotid gland tumors. *J Comput Assist Tomogr* 2007; **31**: 309-316 [PMID: 17414771 DOI: 10.1097/01.rct.0000236418.82395.b3]
 - 14 **Yerli H**, Teksam M, Aydin E, Coskun M, Ozdemir H, Agildere AM. Basal cell adenoma of the parotid gland: dynamic CT and MRI findings. *Br J Radiol* 2005; **78**: 642-645 [PMID: 15961849 DOI: 10.1259/bjr/32453517]
 - 15 **Sakamoto J**, Yoshino N, Okochi K, Imaizumi A, Tetsumura A, Kurohara K, Kurabayashi T. Tissue characterization of head and neck lesions using diffusion-weighted MR imaging with SPLICE. *Eur J Radiol* 2009; **69**: 260-268 [PMID: 18023549 DOI: 10.1016/j.ejrad.2007.10.008]
 - 16 **Jin GQ**, Su DK, Xie D, Zhao W, Liu LD, Zhu XN. Distinguishing benign from malignant parotid gland tumours: low-dose multi-phasic CT protocol with 5-minute delay. *Eur Radiol* 2011; **21**: 1692-1698 [PMID: 21547526 DOI: 10.1007/s00330-011-2101-y]
 - 17 **Lima SS**, Soares AF, de Amorim RF, Freitas Rde A. [Epidemiologic profile of salivary gland neoplasms: analysis of 245 cases]. *Braz J Otorhinolaryngol* 2005; **71**: 335-340 [PMID: 16446938 DOI: 10.1590/S0034-72992005000300012]
 - 18 **de Oliveira FA**, Duarte EC, Taveira CT, Máximo AA, de Aquino EC, Alencar Rde C, Vencio EF. Salivary gland tumor: a review of 599 cases in a Brazilian population. *Head Neck Pathol* 2009; **3**: 271-275 [PMID: 20596844 DOI: 10.1007/s12105-009-0139-9]
 - 19 **Chiu NC**, Wu HM, Chou YH, Li WY, Chiou YY, Guo WY, Chang CY. Basal cell adenoma versus pleomorphic adenoma of the parotid gland: CT findings. *AJR Am J Roentgenol* 2007; **189**: W254-W261 [PMID: 17954621 DOI: 10.2214/AJR.07.2292]
 - 20 **Som PM**. Salivary glands: anatomy and pathology. In: Som PM, ed. *Head and neck imaging*. St. Louis, MO: Mosby, 2003: 2084-2086
 - 21 **de Ru JA**, Plantinga RF, Majoor MH, van Benthem PP, Slootweg PJ, Peeters PH, Hordijk GJ. Warthin's tumour and smoking. *B-ENT* 2005; **1**: 63-66 [PMID: 16044736]
 - 22 **Freedman LS**, Oberman B, Sadetzki S. Using time-dependent covariate analysis to elucidate the relation of smoking history to Warthin's tumor risk. *Am J Epidemiol* 2009; **170**: 1178-1185 [PMID: 19755633 DOI: 10.1093/aje/kwp244]
 - 23 **Hatch RL**, Shah S. Warthin tumor: a common, benign tumor presenting as a highly suspicious mass. *J Am Board Fam Pract* 2005; **18**: 320-322 [PMID: 15994480 DOI: 10.3122/jabfm.18.4.320]
 - 24 **Colella G**, Biondi P, Itró A, Compilato D, Campisi G. Warthin's tumor distribution within the parotid gland. A feasible etiologic source from lymph nodal tissue. *Minerva Stomatol* 2010; **59**: 245-249, 250-252 [PMID: 20502429]
 - 25 **Park CK**, Manning JT, Battifora H, Medeiros LJ. Follicle center lymphoma and Warthin tumor involving the same anatomic site. Report of two cases and review of the literature. *Am J Clin Pathol* 2000; **113**: 113-119 [PMID: 10631864]
 - 26 **Ikeda M**, Motoori K, Hanazawa T, Nagai Y, Yamamoto S, Ueda T, Funatsu H, Ito H. Warthin tumor of the parotid gland: diagnostic value of MR imaging with histopathologic correlation. *AJNR Am J Neuroradiol* 2004; **25**: 1256-1262 [PMID: 15313720]
 - 27 **Burke CJ**, Thomas RH, Howlett D. Imaging the major salivary glands. *Br J Oral Maxillofac Surg* 2011; **49**: 261-269 [PMID: 20381221 DOI: 10.1016/j.bjoms.2010.03.002]
 - 28 **Terada T**. Hyperplastic intraparotid lymph nodes with incipient Warthin's tumor presenting as a parotid tumor. *Pathol Res Pract* 2008; **204**: 863-866 [PMID: 18572328 DOI: 10.1016/j.prp.2008.04.012]
 - 29 **Naujoks C**, Sproll C, Singh DD, Heikaus S, Depprich R, Kübler NR, Handschel J. Bilateral multifocal Warthin's tumors in upper neck lymph nodes. Report of a case and brief review of the literature. *Head Face Med* 2012; **8**: 11 [PMID: 22472434 DOI: 10.1186/1746-160X-8-11]
 - 30 **Teymoortash A**, Schrader C, Shimoda H, Kato S, Werner JA. Evidence of lymphangiogenesis in Warthin's tumor of the parotid gland. *Oral Oncol* 2007; **43**: 614-618 [PMID: 16996778 DOI: 10.1016/j.oraloncology.2006.07.006]
 - 31 **Sharafuddin MJ**, Diemer DP, Levine RS, Thomasson JL, Williams AL. A comparison of MR sequences for lesions of the parotid gland. *AJNR Am J Neuroradiol* 1995; **16**: 1895-1902 [PMID: 8693992]
 - 32 **Som PM**, Biller HF. High-grade malignancies of the parotid gland: identification with MR imaging. *Radiology* 1989; **173**: 823-826 [PMID: 2813793]
 - 33 **Freling NJ**, Molenaar WM, Vermey A, Mooyaart EL, Panders AK, Annyas AA, Thijn CJ. Malignant parotid tumors: clinical use of MR imaging and histologic correlation. *Radiology* 1992; **185**: 691-696 [PMID: 1438746]
 - 34 **Kawata R**, Yoshimura K, Lee K, Araki M, Takenaka H, Tsuji M. Basal cell adenoma of the parotid gland: a clinicopathological study of nine cases--basal cell adenoma versus pleomorphic adenoma and Warthin's tumor. *Eur Arch Otorhinolaryngol* 2010; **267**: 779-783 [PMID: 19908055 DOI: 10.1007/s00405-009-1139-9]
 - 35 **Kakimoto N**, Gamoh S, Tamaki J, Kishino M, Murakami S, Furukawa S. CT and MR images of pleomorphic adenoma in major and minor salivary glands. *Eur J Radiol* 2009; **69**: 464-472 [PMID: 18093776 DOI: 10.1016/j.ejrad.2007.11.021]
 - 36 **Brunese L**, Ciccarelli R, Fucili S, Romeo A, Napolitano G, D' Auria V, Collina A, Califano L, Cappabianca S, Sodano A. Pleomorphic adenoma of parotid gland: delayed enhancement on computed tomography. *Dentomaxillofac Radiol* 2008; **37**: 464-469 [PMID: 19033432 DOI: 10.1259/dmfr/79964183]

P- Reviewer Sheehan JP S- Editor Zhai HH
L- Editor Roemmele A E- Editor Liu XM





百世登

Baishideng®

Published by **Baishideng Publishing Group Co., Limited**

Flat C, 23/F., Lucky Plaza,
315-321 Lockhart Road, Wan Chai,
Hong Kong, China

Fax: +852-65557188

Telephone: +852-31779906

E-mail: bpgoffice@wjgnet.com

<http://www.wjgnet.com>

